Supporting Information

Experimental Section

All chemicals were of analytical grade and purchased from Shanghai Chemical Industrial Corp. and used as received without further purification. A typical synthesis process was as follows.

Synthesis of GeO_2 nanoparticles (np-GeO_2). 0.4 mol of commercial bulk GeO_2 and 0.8 mol of tartaric acid were added into 40 mL ammonium hydroxide in a 60 mL Teflon-lined stainless steel autoclave. Then the autoclave was sealed and maintained at 150 ^{0}C for 6 h after stirred for 1h. After the autoclave was air-cooled to room temperature, the product was filtered and washed with deionized water and ethanol several times, then dried under vacuum at 60 ^{0}C for 6 h. The as-prepared product was heated at 400 ^{0}C for 5 h in air (heating rate 5 ^{0}C min^{-1}).

Synthesis of GeO_2 nanocubes (nc-GeO_2). 0.2 mol of commercial bulk GeO_2 and 0.4 mol of tartaric acid were added into 40 mL ammonium hydroxide in a 60 mL Teflon-lined stainless steel autoclave. Then the autoclave was sealed and maintained at 150 ^{0}C for 6 h after stirred for 1h. After the autoclave was air-cooled to room temperature, the product was filtered and washed with deionized water and ethanol several times, then dried under vacuum at 60 ^{0}C for 6 h. The as-prepared product was heated at 400 ^{0}C for 5 h in air (heating rate 5 ^{0}C min^{-1}).

Synthesis of GeO_2 nanospindles (ns-GeO_2). 0.4 mol of commercial was added into 40 mL ammonium hydroxide in a 60 mL Teflon-lined stainless steel autoclave. Then the autoclave was sealed and maintained at 150 ^{0}C for 6 h after stirred for 1h. After the autoclave was air-cooled to room temperature, the product was filtered and washed with deionized water and ethanol several times, then dried under vacuum at 60 ^{0}C for 6 h. The as-prepared product was heated at 400 ^{0}C for 5 h in air (heating rate 5 ^{0}C min^{-1}).

Material Characterization. The morphology of the reaction product were characterized by scanning electron microscopy (SEM, JEOL-JSM-6700F), Transmission electron microsocopy (TEM, Hitachi H7650 and HRTEM, JEOL 2010). X-ray diffractometer (XRD) was performed on a Philips X' Pert Super diffract meter with Cu Kα radiation (λ=1.54178 Å). The nitrogen adsorption and desorption isotherms were measured with a VELSORP-mini II (BEL Japan, Inc.) at 473 K in the relative pressure range of P/P_0 from 0 to 1 to determine the Brunauer–Emmett–Teller (BET) surface areas and pore size distribution. Raman spectrum was performed with 514.5 nm wavelength to check the compositions and the carbon content of the product was check by EA (Vario EL-III). XPS were recorded on an ESCALAB 250 spectrometer (Perkin-Elmer) to characterize the surface composition.

Electrochemical Measurement. The electrochemical properties of the as-prepared GeO_2 electrodes were measured with coin-type half cells (2016 R-type) which assemble under an argon-filled glove box (H_2O, O_2 < 1 ppm). Working electrode was prepared by mixing the active material, super P carbon black and polyvinylidene fluoride (PVDF) in a weight ratio of 70:20:10. The slurry was pasted onto a Cu foil and then dried in a vacuum oven at 110 ^{0}C for 12 h. The active material density of each cell was determined to be around 1.0~1.5 mg cm^{-2}. Metallic Li sheet was used as counter electrode, and 1 M $LiPF_6$ in ethylene carbonate/dimethylcarbonate (EC/DMC; 1:1 by Volume; Merck) as electrolyte. Galvanostatic measurements were made using a LAND-CT2001A instrument that were cycled between 0.05 V and 1.50 V at a rate of 0.1 – 5 C (1 C = 1000 mA h g^{-1}). Electrochemical impedance spectroscopy (EIS) was carried out on an electrochemical workstation (CHI660D) in the frequency range from 0.1 MHz to 0.01 Hz.

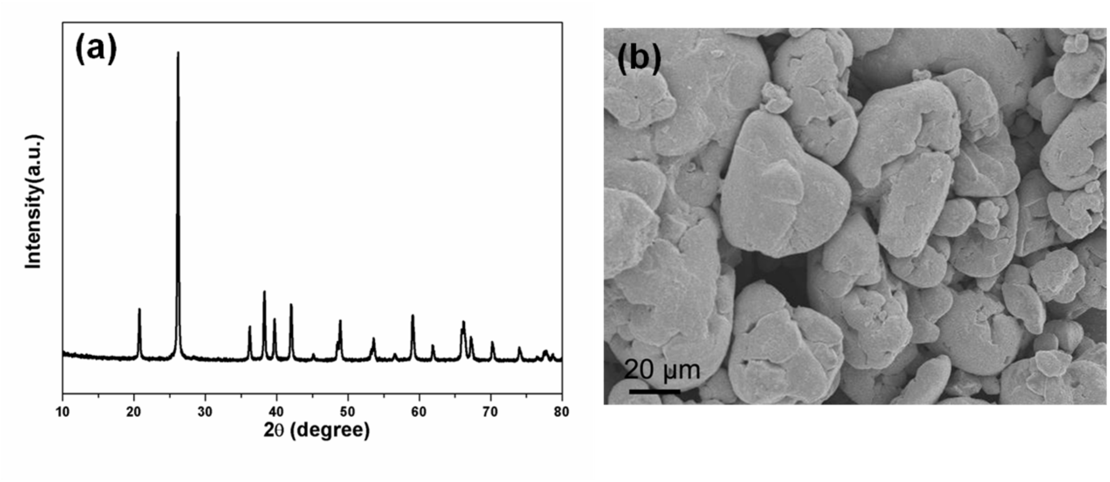

Figure S1. (a) XRD pattern and (b) SEM image of commercial bulk hexagonal GeO_2.

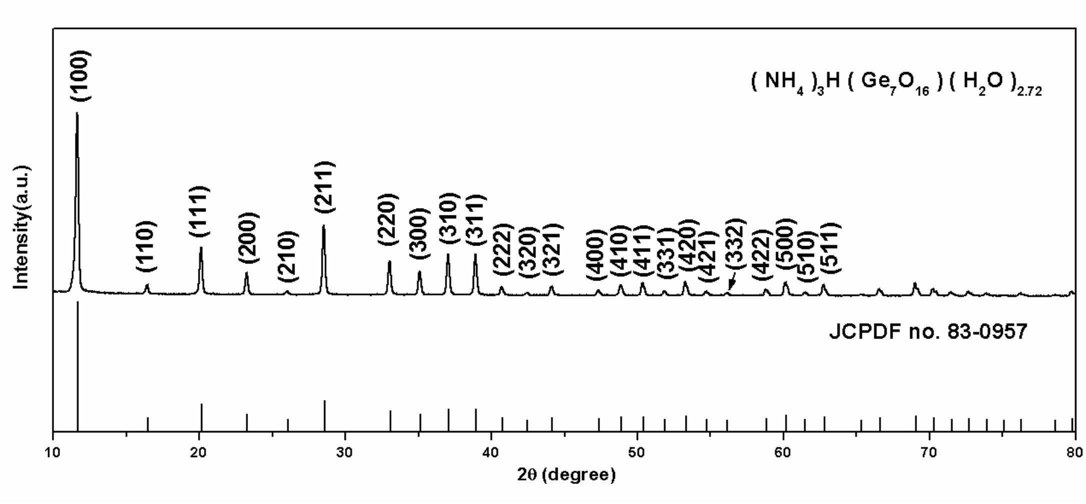

Figure S2. XRD pattern of the as-prepared reacted products under the synthesis temperature of 150 ^{0}C for 6h.

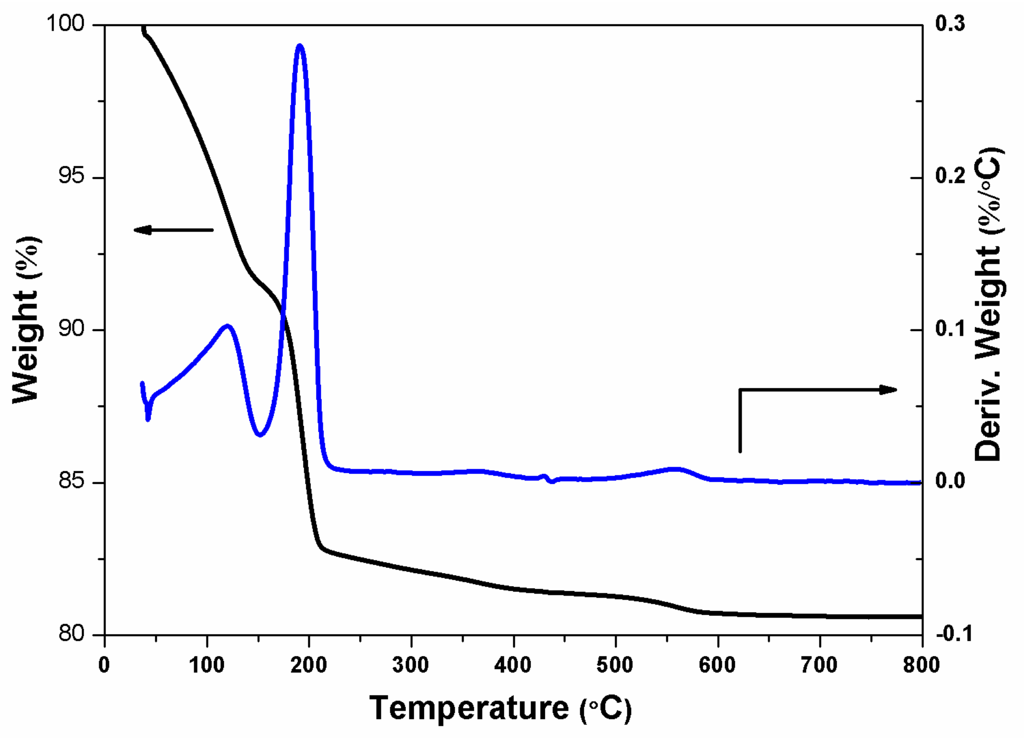

Figure S3. TGA curve of the as-synthesized $(NH_4)_3H(Ge_7O_{16})(H_2O)_{2.72}$ sample.

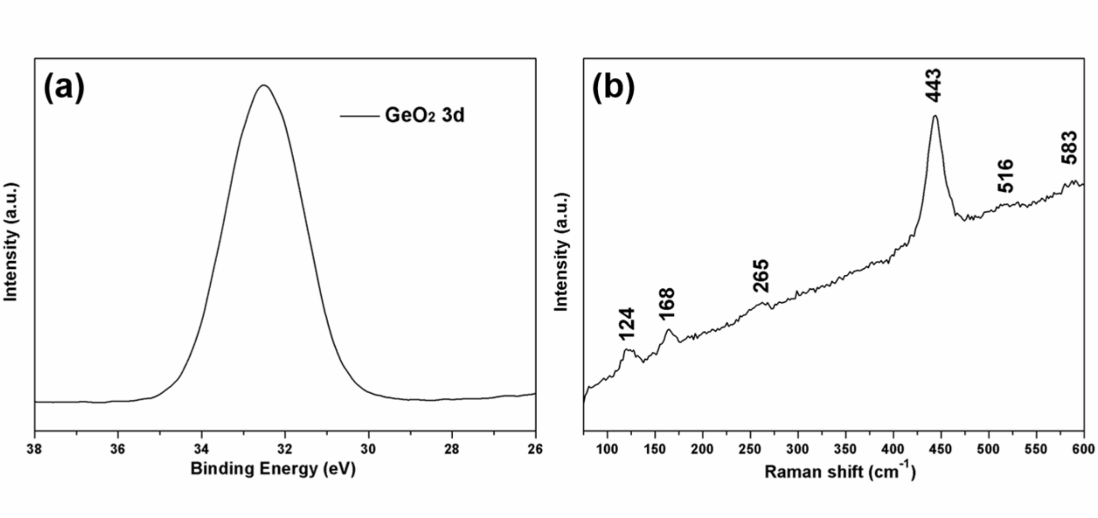

Figure S4. (a) XPS and (b) Raman spectra of the as-prepared GeO_2 nanoparticles.

The Ge3d spectrum shown in Figure S4a exhibits the Ge3d5/2 peak at 32.3 eV due to the Ge−O bond in GeO_2, which is consistent with the chemical composition of GeO_2. The Raman spectrum in Figure S3b shows six distinct peaks centered at 124 cm^{-1}, 168 cm^{-1}, 265 cm^{-1}, 443 cm^{-1}, 516 cm^{-1}, and 583 cm^{-1}, which is correlated to the vibration modes of E(LO + TO), E(LO + TO), A_1, A1 (high), E(LO) and E (TO), respectively. These results are consistent with the reported results for α- GeO_2.[1]

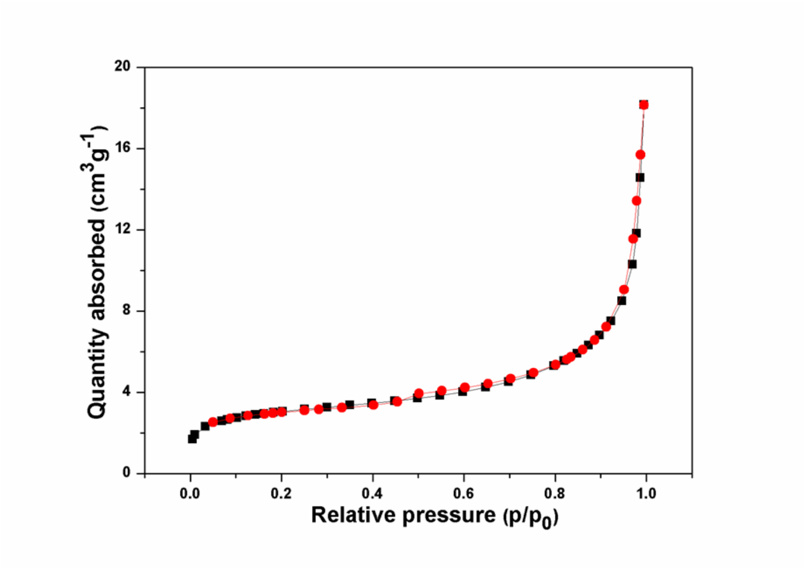

Figure S5. Nitrogen adsorption and desorption isotherms of np-GeO_2.

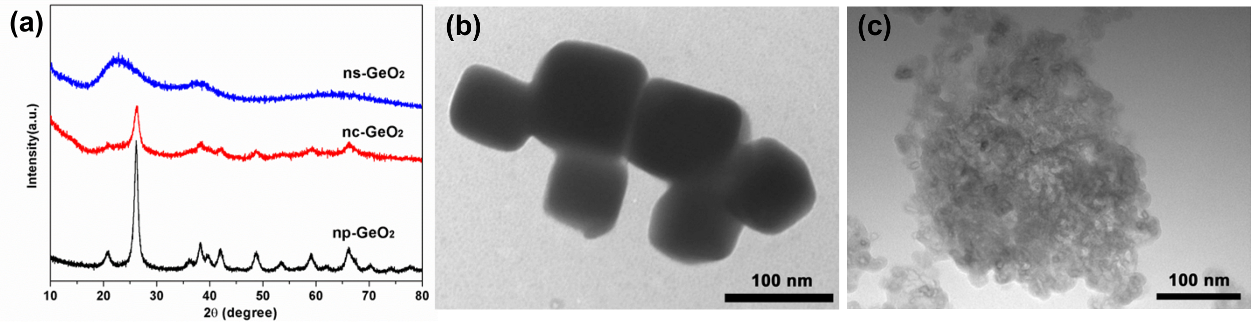

Figure S6. (a) XRD patterns of the three GeO_2 samples. TEM images of as-prepared b) GeO_2 nanocubes and c) GeO_2 nanospindles.

Figure S6a shows the XRD patterns of the three as-prepared GeO_2 samples. And it is obvious that diffraction peaks broadening occurs for the ns-GeO_2 and nc-GeO_2 samples, indicating the smaller size of the particles of these two samples. The size information of np-GeO_2 sample is about 200nm as shown in the SEM and TEM images. The size of the nc-GeO_2 sample estimated by the Scherrer equation was about 70nm. For the ns-GeO_2 sample, its XRD pattern shows the formation of amorphous-like phase, and its size was further determined from TEM image in Figure S6c, from which one can see that this sample is assembled by much smaller nanoparticles about several nanometers.

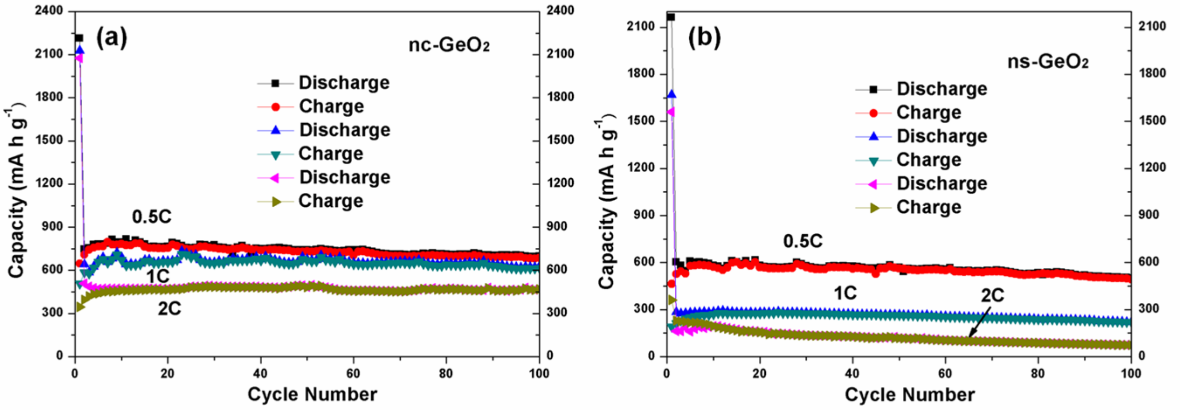

Figure S7. Cycling performance of commercial nc-GeO_2 and ns-GeO_2 at the current rate of 0.5, 1, and 2 C.

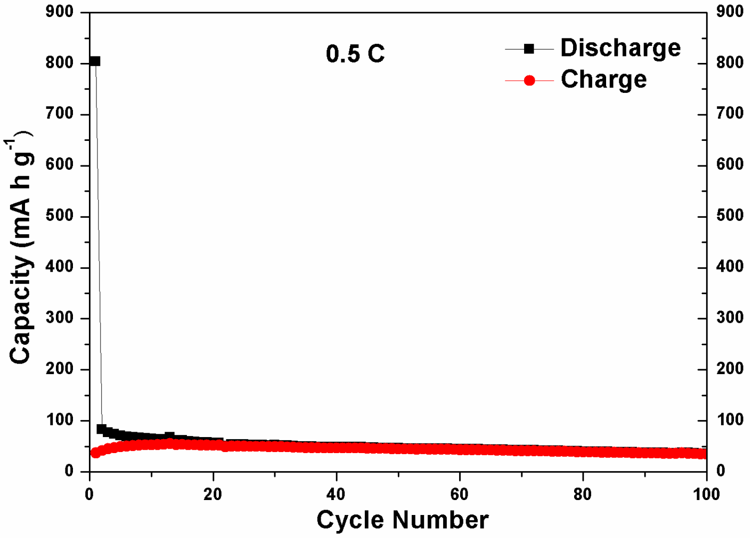

Figure S8. Cycling performance of commercial bulk GeO_2 at the current of 0.5 C.

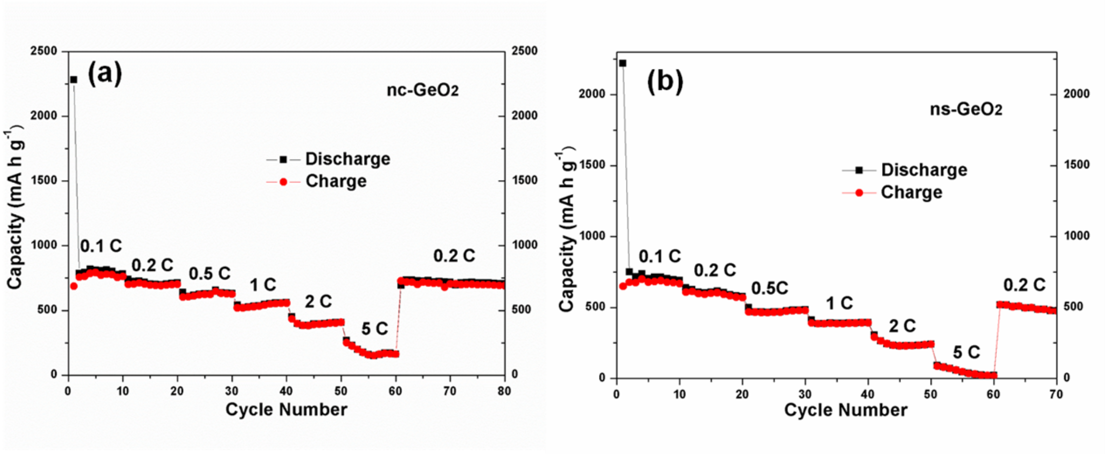

Figure S9. Rate capabilities and cycling performance of nc-GeO_2 and ns-GeO_2 at various C rates.

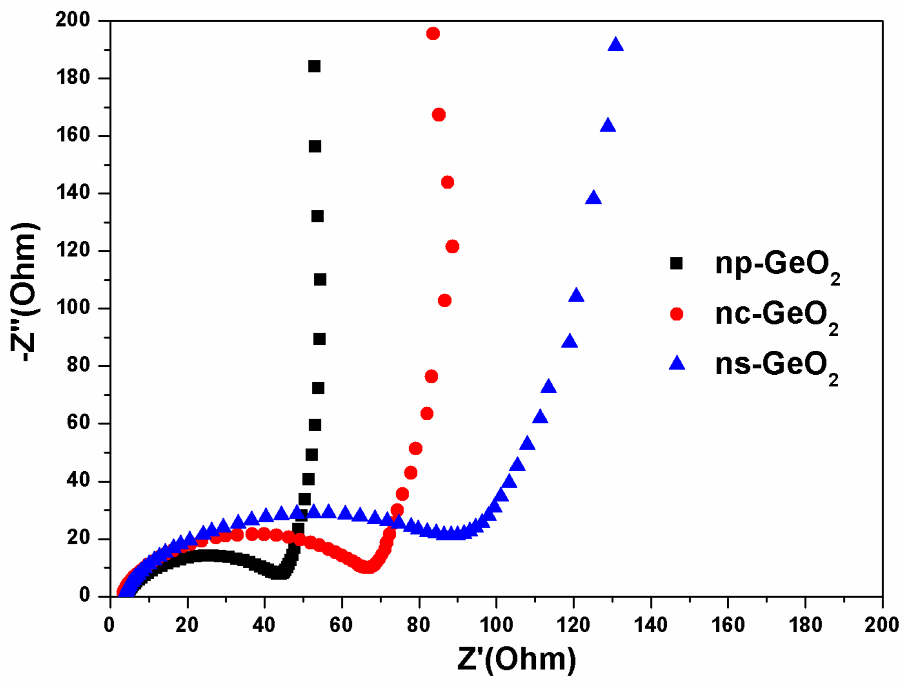

Figure S10. Electrochemical impedance spectroscopy of GeO_2 electrodes.

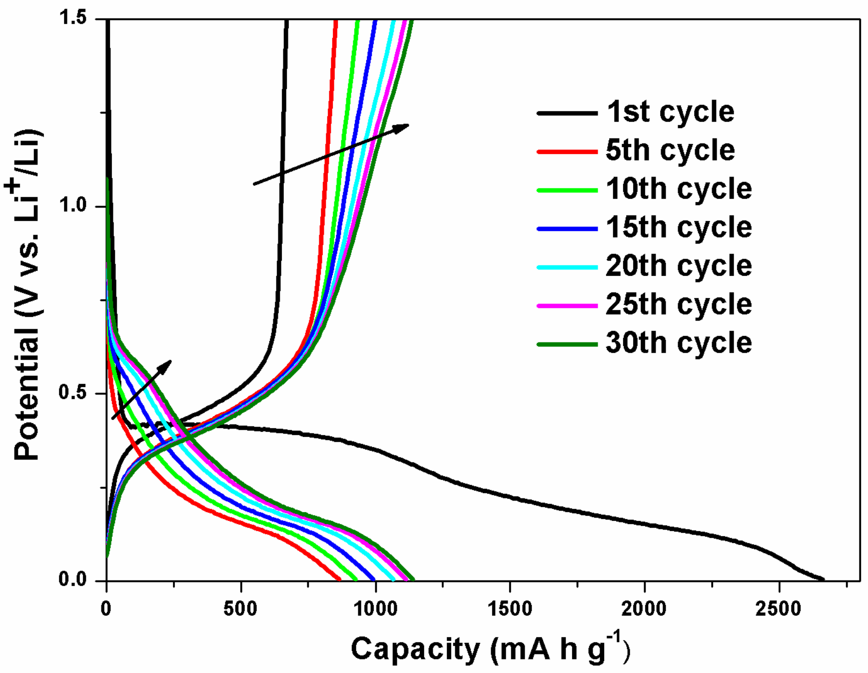

Figure S11. Galvanostatic charge-discharge voltage profiles for np-GeO_2 cycled at a rate of 0.5 C between 1.5 and 0.05 V versus Li^+/Li.

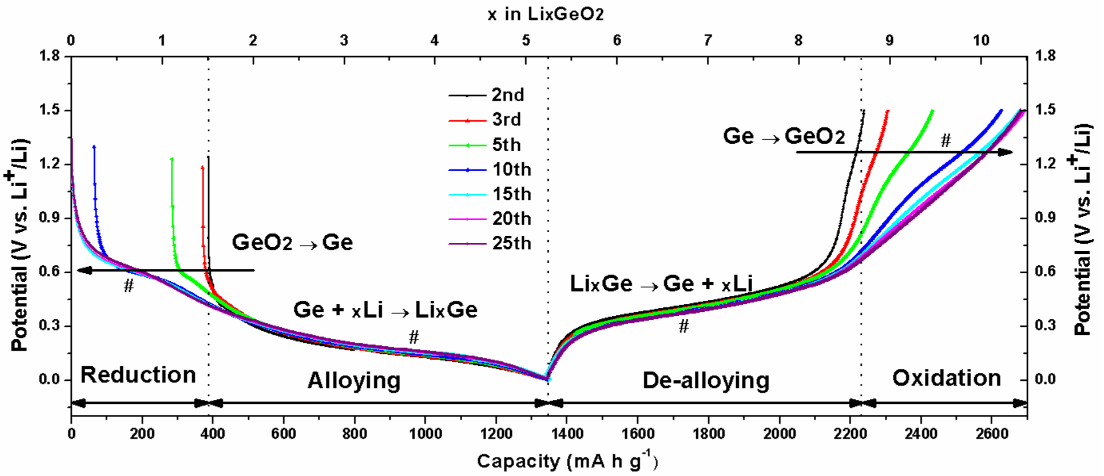

Figure S12. Discharge–charge voltage profiles of the np-GeO_2 at 0.1 C in the voltage window of 0.005-1.5 V (vs. Li^+/Li) at room temperature. Vertical lines indicate the expected capacities for the alloying/de-alloying process and partial reduction-oxidation of GeO_2 (reduction at ~ 0.6 V and oxidation at ~ 1.3 V), respectively.

It's worth mentioning that the reversible capacity of np-GeO_2 at 0.1 C is much higher than the theoretical capacity of 1126 mA h g^{-1} for GeO_2, which has not been reported before. Figure S12 shows the discharge-charge voltage profiles of the np-GeO_2 at 0.1 C. For the discharge curves on the left we can see that: (1) in the 2nd cycle, the discharge capacity of 959 mA h g^{-1} is mostly contributed by the alloying process, corresponding to about 3.77 Li^+ involved in. (2) the discharge capacities due to the alloying process are almost the same from 2nd to 25th cycle, while more capacities, caused by partial reduction of the re-oxidized GeO_2, appear gradually. The maximal of such capacity is about 390 mA h g^{-1} (about 1.5 Li^+) since 15th cycle, and the discharge curves overlap together afterwards. Therefore, the total amount of Li^+ during discharging process is 5.27 Li^+ per GeO_2, indicating higher discharge capacity can be obtained than theoretical. Moreover, the de-alloying and partial oxidation processes which are showed in the charge curves on the right, match well with the reaction during discharge and further explain the higher reversible capacities obtained in our study.

References

S1. T. P. Mernagh and L.-g. Liu, *Physics and chemistry of minerals*, 1997, **24**, 7-16.